Control of Attenuation Pole Frequency of a Dual-Mode Microstrip Ring Resonator Bandpass Filter

Arun Chandra Kundu, *Member, IEEE,* and Ikuo Awai, *Member, IEEE*

***Abstract*—A novel method is proposed to control the attenuation pole frequency of a dual-mode circular microstrip ring resonator bandpass filter, keeping the bandwidth constant. In this paper, the coupling between the dual modes is provided as the total effect of stub perturbation at the end of symmetry plane, and the angle between input/output ports. By making a various combinations of these two parameters, it is possible to control the attenuation pole frequency. An additional small coupling induced by excitation capacitance is also considered. Filters are simulated using the calculated coupling constant, and then the attenuation pole frequencies and bandwidth of the simulated filters are verified by experiment. Theoretical expressions are further devised to calculate the attenuation pole frequencies.**

***Index Terms*—Attenuation pole frequency, bandpass filter, bandwidth, coupling, dual mode, filter frequency, ring resonator.**

I. Introduction

AS IS WELL known, use of a dual-mode resonator allows the realization of a compact high-quality microwave bandpass filter (BPF) and its attenuation poles play a vital role in improving the skirt characteristics. Control of attenuation pole frequency of a BPF with a constant bandwidth will open a new door in the design of a BPF.

There have been many studies on dual-mode ring resonator BPFs because a ring resonator has much potential for variety of applications together with its simple structure [1]. However, until today, few papers have been published regarding the attenuation pole frequency control of a dual-mode BPF [2]–[5]. Reference [2] presents one of a few examples, though the attenuation pole frequency changes within a small range, thus, disregarding the circuit matching. In our previous papers, we have controlled the attenuation pole frequency of a dual-mode microstrip circular disk resonator by making a combination of two stub perturbations placed along the symmetry plane, keeping the total perturbation constant [3], [4]. However, we were able to control the attenuation pole frequency only in a narrow range by this method. In [5], some experimental data are presented regarding attenuation pole frequency control of a dual-mode dielectric waveguide resonator BPF, where the position of the higher attenuation pole frequency remain almost unchanged, although the position of the lower attenuation pole frequency is shifted with respect to the position of excitation electrodes.

In this paper, we will propose a new method to control the attenuation pole frequencies over a wide range by making a various combination of stub perturbation and excitation angle. Coupling between the two degenerate modes can be kept constant by decreasing the stub perturbation and excitation angle at the same time. In fact, decrease of stub perturbation reduces the internal coupling between the dual modes. The excitation angle also has an effect to internal coupling, i.e., coupling induced by the I/O port impedance increases with the decrease of the I/O angle, while the attenuation poles' frequency changes differently according to the two above-mentioned coupling schemes. As a result, we can create a combination of these two parameters to obtain a constant coupling for design of a constant bandwidth filter with controlled attenuation pole frequencies. New theoretical expressions are devised for coupling constant and attenuation pole frequencies. The calculated results are verified by experiment and simulation. A unique, but complicating (second order), effect of external circuit susceptance is also included to characterize the coupling constant.

II. Coupling Constant

The external circuit susceptance and angular position of the I/O terminal contribute to internal coupling between two resonant modes in addition to the stub perturbation [6]. Considering these three factors, we have devised a theory for coupling constant as follows.

The configuration and schematic diagram of a microstrip ring resonator are shown in Figs. 1 and 2, respectively, where a_1 and a_2 are the outer and inner radii of the ring resonator, respectively. The thickness and relative dielectric constant of the substrate are 1.6 mm and 10.5, respectively. Capacitive stub perturbations having a width and length of w and d, respectively, are placed at the end of symmetry plane, which also contributes to the appearance of attenuation poles at both sides of the passband [6]. For even-mode resonant frequency calculation, the symmetry plane in Fig. 2 will act as an open end, i.e., as a perfect magnetic wall, and the equivalent transmission-line circuit of Fig. 2 will become as shown in Fig. 3. Thus, we can write

$$y_1 = \frac{jb_{\mathrm{p}} + j2\tan\beta(l-x)}{2 - b_{\mathrm{p}}\tan\beta(l-x)} \tag{1}$$

$$y_2 = jb_{\mathrm{e}} + \frac{jb_{\mathrm{p}} + j2\tan\beta x}{2 - b_{\mathrm{p}}\tan\beta x} \tag{2}$$

Manuscript received December 9, 1999; revised October 26, 2000.

A. C. Kundu is with the Telecom Technology Development Center, TDK Corporation, Chiba 272-8558, Japan.

I. Awai is with the Department of Electrical and Electronic Engineering, Yamaguchi University, Yamaguchi 755-8611, Japan.

Publisher Item Identifier S 0018-9480(01)03979-5.

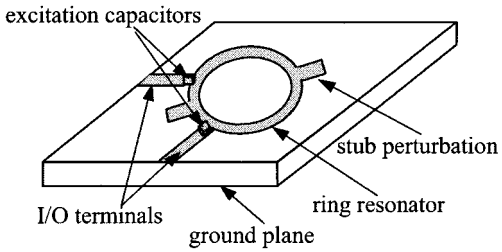

Fig. 1. Configuration of a microstrip ring resonator.

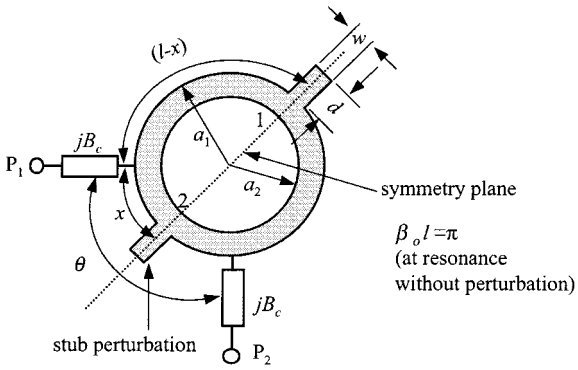

Fig. 2. Schematic diagram of a microstrip ring resonator ($a_1 = 9.7$ mm, $a_2 = 7$ mm, $\varepsilon_r = 10.5$).

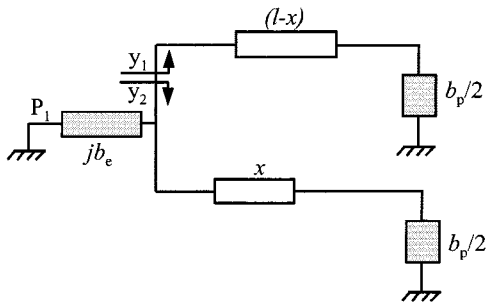

Fig. 3. Equivalent transmission-line circuit model for even-mode calculation (The characteristic impedance of the transmission line is taken to be one).

where b_e is $(G_0 b_c)/Y_a$ (the terms Y_a, b_c, and G_0 will be defined in Section III), y_1 and y_2 are input admittances at the reference plane, β is the propagation constant, l is πa ($a =$ the average of a_1 and a_2), and b_p is the normalized perturbation susceptance, which can be defined as [2]

$$b_p = \frac{Y_b}{Y_a} \tan \beta_0 d \tag{3}$$

where β_0 is $(\omega_0 \sqrt{\varepsilon_{eff}})/c$, ω_0 is the angular resonant frequency, Y_b is the characteristic admittance of the perturbation stub, ε_{eff} is the effective dielectric constant, c is the velocity of light in free space, and β_0 is the propagation constant without perturbation. ε_{eff} can be defined as [7]

$$\varepsilon_{eff} = \frac{\varepsilon_r + 1}{2} + \frac{\varepsilon_r - 1}{2} \left(1 + \frac{10h}{w}\right)^{-0.5} \tag{4}$$

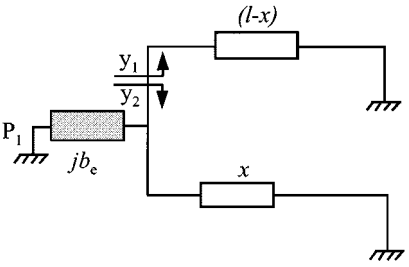

Fig. 4. Equivalent transmission-line circuit model for odd-mode calculation.

where ε_r is the dielectric constant of the microstrip resonator, w is the width of the perturbation stub, and h is the thickness of the substrate.

At resonance

$$y_1 + y_2 = 0. \tag{5}$$

Let us suppose that $\beta = \beta_o + \Delta\beta_e$. In other words, the resonant frequency is shifted a little from the original resonance condition due to the perturbations. The propagation constant β is used here to represent the resonant frequency. By using Taylor series expansion and doing some manipulations of (5), we get the following relation for calculation of even-mode resonant frequency by neglecting the terms of higher order than $\Delta\beta_e^2$:

$$\begin{aligned}\Delta\beta_e^2 \Big[& A(2lx - l^2) \tan\beta_0 x \sec^2 \beta_0 x - B(l-x)^2 \tan^2 \beta_0 x \\ & \times \sec^2 \beta_0 x \Big] + \Delta\beta_e^2 \Big[B(xl - x^2) \sec^4 \beta_0 x \\ & - Bx^2 \tan^2 \beta_0 x \sec^2 \beta_0 x \Big] \\ & + \Delta\beta_e \Big[Al \sec^2 \beta_0 x + B(l - 2x) \tan\beta_0 x \sec^2 \beta_0 x \Big] \\ & + C - B \tan^2 \beta_0 x = 0 \end{aligned} \tag{6}$$

where

$$\begin{aligned} A &= -b_p^2 - 2b_p b_e + 4 \\ B &= -4b_p + b_p^2 b_e \end{aligned}$$

and

$$C = 4(b_p + b_e)$$

and $\Delta\beta_e$ is the change of the even-mode propagation constant.

For odd-mode resonant frequency, the symmetry plane of Fig. 2 will simply be short circuited, i.e., act as a perfect electric wall, as shown in Fig. 4, and we can obtain the following relation for the odd-mode propagation constant:

$$\begin{aligned} -\Delta\beta_o^2 (2lx - l^2) \cot\beta_0 x \operatorname{cosec}^2 \beta_0 x \\ + \Delta\beta_o l \operatorname{cosec}^2 \beta_0 x + b_e = 0 \end{aligned} \tag{7}$$

where $\Delta\beta_o$ is the change of the odd-mode propagation constant. Hence, the coupling constant can be calculated using the following relation:

$$k = \frac{2|\Delta\omega_e - \Delta\omega_o|}{2\omega_0 + \Delta\omega_e + \Delta\omega_o} = \frac{2|\Delta\beta_e - \Delta\beta_o|}{2\beta_0 + \Delta\beta_e + \Delta\beta_o}. \tag{8}$$

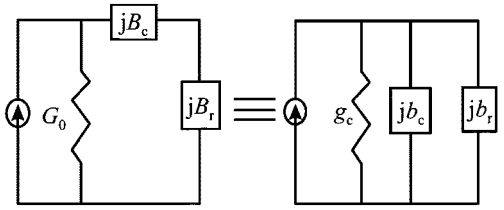

Fig. 5. Connection of a resonator with external circuit via susceptance.

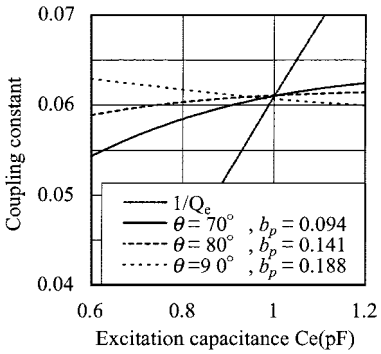

Fig. 6. Coupling constant versus excitation capacitance of a ring resonator ($f = 2.08$ GHz, $Y_{\rm a} = 0.0283$).

III. Resonant Frequency and External Quality Factor

The unperturbed resonant frequency of the dominant mode of a microstrip ring resonator can be calculated using the following relation [1]:

$$f_0 = \frac{c}{2\pi a\sqrt{\varepsilon_{\rm eff}}} \tag{9}$$

where c is the velocity of light in free space, a is the average of the outer and inner radii of the ring resonator, and $\varepsilon_{\rm eff}$ is the effective dielectric constant.

When a circular microstrip ring resonator is connected to external circuits via a series susceptance, as shown in Fig. 1, the external quality factor $(Q_{\rm e})$ can be calculated by use of the equivalence shown in Fig. 5 and expressed by the following equation [4]:

$$Q_{\rm e} = \frac{1}{g_c}\left(b_c + \frac{\pi Y_{\rm a}}{G_0}\right) \tag{10}$$

where $g_c = B_c^2/(G_0^2 + B_c^2)$, $b_c = G_0 B_c/(G_0^2 + B_c^2)$, $B_c = \omega_0 C_{\rm e}$, $C_{\rm e}$ is the excitation capacitance, $Y_{\rm a}$ is the characteristic admittance of the ring resonator transmission line, G_0 is the characteristic admittance of the external circuit, and ω_0 is the angular resonant frequency.

By taking the reciprocal of $Q_{\rm e}$, we can calculate the external circuit coupling with the variation of excitation capacitance $C_{\rm e}$. The calculated result is shown in Fig. 6. From this figure, we observe that the reciprocal of $Q_{\rm e}$ increases with $C_{\rm e}$ monotonically.

Now, as an example, we will design a two-pole Butterworth BPF of relative bandwidth 8.6% (resonant frequency of the microstrip ring resonator without perturbation is 2.08 GHz). We know it requires the coupling constant 0.061 and, thus, $C_{\rm e} = 1$ pF has to be chosen referring to Fig. 6. Hence, for I/O angles of 90°, 80°, and 70°, we have tried to find out a coupling constant of 0.061 at $C_{\rm e} = 1$ pF for various values of stub perturbations, which are also shown in Fig. 6. From this figure, we observe that when the I/O angle is decreasing from 90° to 70°, the amount of stub susceptance required to produce the same amount of coupling is decreasing, i.e., the amount of internal coupling contributed by the I/O terminal is increasing [6]. By averaging the even- and odd-mode frequencies, we can calculate the filter center frequency.

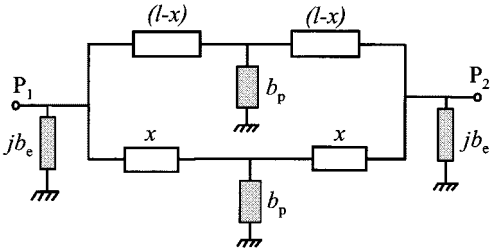

Fig. 7. Transmission-line equivalent-circuit model of the BPF for simulation.

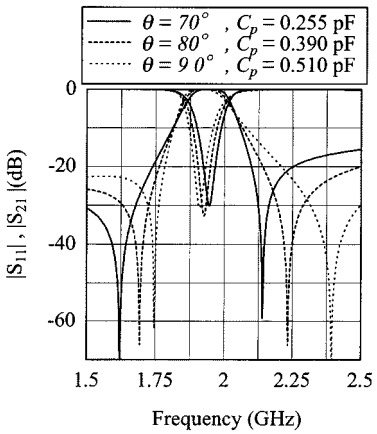

Fig. 8. Simulated responses of the filters explaining attenuation pole frequency control.

IV. Simulation and Fabrication of BPFs

The transmission-line equivalent circuit of the ring resonator BPF is shown in Fig. 7, where $b_{\rm p}$ is the normalized total stub perturbation at each symmetry end, $b_{\rm e}$ is the external circuit susceptance, and P_1 and P_2 are the I/O terminals. We have simulated this circuit by using the calculated circuit parameters for various combinations, as discussed earlier [4]. The equivalent perturbation capacitance $C_{\rm p}$ is calculated by using the following well-known equation:

$$b_{\rm p} = \omega_0 C_{\rm p}. \tag{11}$$

The response of simulated filter is shown in Fig. 8. The circuit simulation was performed by using the Advanced Design System (ADS), Agilent Technology, Tokyo, Japan. From this figure, we observe that both of the attenuation poles are shifted toward higher frequencies with an increase in the amount of stub susceptance. Since the total amount of internal coupling remains constant, the bandwidth remains the same in each case. The response of a fabricated filter is shown in Fig. 9, which shows a very good agreement with the simulated responses of Fig. 8.

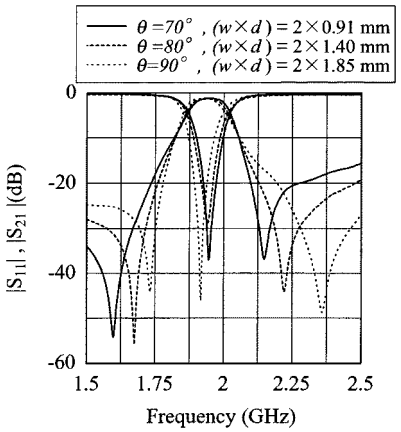

Fig. 9. Measured results for attenuation pole frequency control.

TABLE I
EXPERIMENTAL, SIMULATED, AND THEORETICAL FILTER CENTER FREQUENCIES

θ	Experimental (MHz)	Simulated (MHz)	Theoretical (MHz)
90°	1927	1910	1906
80°	1937	1922	1924
70°	1944	1940	1943

Since losses are not considered in simulation, there is a little discrepancy between the decibel value of the attenuation pole dip in simulated and experimental results. Due to the increase of the amount of the stub susceptance (which acts as a parallel capacitance with the resonator) with the increase of the I/O angle, the filter center frequency is slightly decreasing in each case [4]. The experimental, simulated, and theoretical filter center frequencies are shown in Table I, which are in good agreement.

V. ATTENUATION POLE FREQUENCIES

Referring to Fig. 7, the condition for appearance of attenuation poles at both sides of the passband of a ring resonator model, which is described by a model having two branch lines from input to output, can be given as [3]

$$y_{21}^{(1)} + y_{21}^{(2)} = 0 \tag{12}$$

where

$$y_{21}^{(1)} = \frac{j}{\left[\sin\beta(l-x)\left\{2\cos\beta(l-x) - b_{\rm p}\sin\beta(l-x)\right\}\right]}$$

and

$$y_{21}^{(2)} = \frac{j}{\left[\sin\beta x\left\{2\cos\beta x - b_{\rm p}\sin\beta x\right\}\right]}.$$

By following the same calculation procedure as in Section II, we have the following relation to calculate the attenuation pole frequencies using (12):

$$\Delta\beta^2\left[\left(2l^2-4lx\right)\sin 2\beta_0 x+\left(2b_{\rm p}lx-b_{\rm p}l^2-2b_{\rm p}x^2\right)\cos 2\beta_0 x\right] +\Delta\beta\left[\left(b_{\rm p}l-2b_{\rm p}x\right)\sin 2\beta_0 x+2l\cos 2\beta_0 x\right]-2b_{\rm p}\sin^2\beta_0 x = 0. \tag{13}$$

TABLE II
EXPERIMENTAL, SIMULATED, AND THEORETICAL ATTENUATION POLE FREQUENCIES

θ		f_h (MHz)	f_l (MHz)
90°	Exp.	2359	1732
	Simu.	2374	1746
	Theo.	2325	1741
80°	Exp.	2220	1675
	Simu.	2234	1693
	Theo.	2198	1672
70°	Exp.	2149	1597
	Simu.	2140	1622
	Theo.	2126	1573

Since (13) is a quadratic equation, we can get two values of $\Delta\beta$ ($\Delta\beta_{\rm h}$ and $\Delta\beta_{\rm l}$) corresponding to higher and lower attenuation pole frequencies. Hence,

$$f_{\rm h} = f_0\left[1+\frac{\Delta\beta_{\rm h}}{\beta_0}\right] \tag{14}$$

and

$$f_{\rm l} = f_0\left[1+\frac{\Delta\beta_{\rm l}}{\beta_0}\right] \tag{15}$$

where $f_{\rm h}$ and $f_{\rm l}$ are the higher and lower attenuation pole frequencies, respectively. The calculated, simulated, and measured attenuation pole frequencies are in good agreement with each other, as shown in Table II.

VI. CONCLUSION

In this paper, we have successfully controlled the attenuation pole frequencies of a dual-mode circular microstrip ring resonator BPF keeping the bandwidth constant. A theory to calculate the coupling constant has been devised. The reason for little variation in the filter center frequency has been illustrated. The equation to calculate the attenuation pole frequency has been explained. The theory presented in this paper is not limited to a circular microstrip or ring resonator structure, but will be similarly applied to any circular dual-mode resonator BPF, as shown in [4]. The wide range control of attenuation pole frequency also opens a new door for designing a duplexer within the desired band, with minimum overlapping or without overlapping of the transmission characteristics, since the sharpness of the skirt characteristics of the BPF can be controlled over a wide range.

REFERENCES

[1] K. Chang, *Microwave Ring Circuits and Antennas*. New York: Wiley, 1996.
[2] L. Zhu and K. Wu, "A joint field/circuit design model of microstrip ring dual-mode filter: Theory and experiments," in *Asia–Pacific Microwave Conf.*, 1997, pp. 865–868.
[3] A. C. Kundu, I. Awai, and Y. Osako, "Explanation and control of attenuation poles in a microstrip circular disk resonator bandpass filter," IEICE, Tokyo, Japan, Tech. Rep. MW98–16, May 1998.
[4] I. Awai, "General theory of a circular dual-mode resonator and filter" (in Japanese), *IEICE Trans. Electron.*, vol. E81-C, no. 1, pp. 1575–1763, Nov. 1998.

[5] I. Awai, A. C. Kundu, and T. Yamashita, "Equivalent circuit representation and explanation of attenuation pole of a dual- mode dielectric resonator bandpass filter," *IEEE Trans. Microwave Theory Tech.*, vol. 46, pp. 2159–2163, Dec. 1998.
[6] I. Awai and T. Yamashita, "Theory on rotated excitation of a circular dual-mode resonator and filter," in *IEEE MTT-S Int. Microwave Symp. Dig.*, vol. 45, June 1997, pp. 781–784.
[7] M. V. Schneider, "Microstrip lines for microwave integrated circuits," *Bell Syst. Tech. J.*, vol. 48, pp. 1421–1444, May 1969.

Arun Chandra Kundu (S'94-A'96–M'99) was born in Rajbari, Bangladesh. He received the B.S.E.E. degree from the Bangladesh University of Engineering and Technology (BUET), Dhaka, Bangladesh, in 1989, and the M.S.E.E. and Dr. Eng. degrees from Yamaguchi University, Yamaguchi, Japan in 1996 and 1999 respectively.

In April 1999, he joined the TDK Corporation, Chiba, Japan, where he is currently a Senior Research and Development Engineer. His current research interest is focused on microwave dielectric waveguide devices for advanced mobile communication systems.

Dr. Kundu is a member of the IEEE Microwave Theory and Techniques Society (IEEE MTT-S). He was the recipient of the 2000 Research Directors Special Award of Excellent Invention presented by the TDK Corporation.

Ikuo Awai (M'78) received the B.S., M.S., and Ph.D. degrees from Kyoto University, Kyoto, Japan, in 1963, 1965, and 1978, respectively.

In 1968, he joined the Department of Electronics, Kyoto University, as a Research Associate, where he was engaged in microwave magnetic waves and integrated optics. From 1984 to 1990, he was with the Uniden Corporation, where he developed microwave communication equipment. In 1990, he joined Yamaguchi University, Yamaguchi, Japan, as a Professor, where he has studied magnetostatic wave devices, dielectric waveguide components, and superconducting devices for microwave application.

Dr. Awai is a member of the IEEE Microwave Theory and Techniques Society (IEEE MTT-S), the IEEE Antennas and Propagation Society (IEEE AP-S), and the IEEE Magnetostatic Society.